DOI: 10.1021/acs.jpcc.8b08126

A Second Order Cumulant Approach for the Evaluation of Anisotropic Hole Mobility in Organic Semiconductors

Alessandro Landi,*,† Raffaele Borrelli,‡ Amedeo Capobianco,† Amalia Velardo,† and Andrea Peluso†

†*Dipartimento di Chimica e Biologia Adolfo Zambelli, Università di Salerno, Via Giovanni Paolo II, I-84084 Fisciano (SA), Italy*

‡*Department of Agricultural, Forestry and Food Science, University of Torino, I-10195 Grugliasco, Italy*

E-mail: alelandi1@unisa.it

DOI: 10.1021/acs.jpcc.8b08126

Abstract

The anisotropic field effect mobilities of four prototypical semiconducting materials, i.e. single crystals of pentacene, tetracene, picene, and rubrene, are evaluated by using the hopping model with time averaged rates obtained at the second-order cumulant (SOC) expansion of the time dependent reduced density matrix. It is shown that the SOC approach allows for correcting the two known failures of the hopping mechanism: the highly overestimated mobilities provided by the Fermi Golden Rule and the incorrect temperature dependence predicted by the semiclassical Marcus approach.

Introduction

Molecular electronics should hopefully lead toward making small-sized flexible devices, constituted by less expensive and easy to handle materials. Organic semiconductors have the properties to fit these requests: with respect to their inorganic counterparts, they can be processed at lower temperatures, exhibit good mechanical properties such as high flexibility and strength; furthermore, their chemico-physical properties can be easily tuned by using different functional groups.[1–3] Organic materials are currently used in organic field-effect transistors (OFET),[4] organic light emitting diodes (OLED),[5] and organic solar cells (OSC).[6] Even though research in this field is still very active, progresses have been somewhat slowed down by the limited understanding of the charge transport properties of organic materials. Indeed, there is still debate about the most appropriate theoretical approach to model charge transport in organic semiconductors, especially for high-mobility molecular semiconductors, which exhibit mobilities larger than ≈ 1 $cm^2V^{-1}s^{-1}$. Since organic molecular crystals are only weakly bound by van der Waals interactions, lattice vibrations play a more important role in organic than in inorganic materials.[7,8] The occurrence of vibrational effects makes neither the hopping nor the band-like mechanism adequate for treating charge transport in organic semiconductors.[7,9–14] On one hand, hopping, usually used in conjunction with rate constants obtained by Marcus theory, predicts a thermally activated mechanism not

DOI: 10.1021/acs.jpcc.8b08126

fully consistent with experimental observations.[15] On the other hand, a genuine band-like mechanism is ruled out by the short mean free path observed in OFET.[16]

Several alternative models have been proposed, based on Ehrenfest dynamics,[17] modified surface hopping,[18] open quantum systems dynamics,[19] many-body physics methods[20] relying both on model Hamiltonians[21] and realistic chemical models.[13,14,22–24] According to a recently proposed theoretical approach, the unavoidable disorder in real crystals leads to a "transient localization" which would severely slow down carrier mobility. nevertheless, time fluctuations of crystal disorder may still activate charge diffusion.[16,25]

However, both theoretical estimations[11] and experimental measurements[26] of mobility carried out at different temperatures show that the hopping model is adequate for the evaluation of charge mobility, at least at room temperature. Moreover both localized (Marcus) and semiclassical dynamics models predict quite similar mobilities, even if charge delocalization at room temperature is considered.[27] In addition, thermal motions in organic crystals give rise to enhanced molecular distortion, leading in turn to strong fluctuations in the transfer integral,[9] thus breaking the translational symmetry of the electronic Hamiltonian and causing a localization of the charge carriers. That occurs also in pentacene, despite the low reorganization energy and large transfer integrals.[28] Finally, it has been pointed out that the inclusion of quantum mechanical effects in the hopping rates does not lead to thermally activated mobilities.[28,29] That is an important point, indeed the hopping mechanism can not be ruled out only on the basis of the observed decreasing of the mobility with temperature. Nevertheless, quantum based models such as the Fermi's Golden rule (FGR), strongly overestimate hole mobilities for most of organic semiconductors, even high-mobility ones, possibly because of the intrinsic limits of FGR in treating ultrafast transitions.[30]

Herein we consider an alternative approach for deriving hopping rate constants, based on the second-order cumulant expansion of the time dependent reduced density matrix (SOC),[31] which appears to solve both the incorrect temperature dependence and the unphysically oversrestimation of hole mobilities. The SOC model is a full quantum mechanical approach

DOI: 10.1021/acs.jpcc.8b08126

which should provide a significant improvement with respect to FGR, inasmuch as it does not require the use of integral representation of the Dirac delta function and, unlike FGR, allows to take into account the change of the reaction rate with time, describing the population $P(t)$ of the state of interest as:

$$\frac{\mathrm{d}P(t)}{\mathrm{d}t} = k(t)P(t). \tag{1}$$

We use a well recognized protocol[32] which expresses the mobility of organic semiconductors for each direction in terms of angles between the charge-hopping pathways and the plane of interest[33,34] for 4 prototypical organic semiconducting molecules: pentacene, tetracene, picene and rubrene, chosen because of their relatively high experimental mobilities.[35] Results obtained by using SOC approach are also compared with FGR and Marcus predictions of rate constants. It is shown that, within the limits of the simple hopping mechanism, SOC approach provides reliable hole mobilities. In particular, at variance with other tested methodologies, the SOC approach is able to predict a temperature dependence in line with the experimental results.

Theory and modeling

Fermi's golden rule

Full mode quantum charge transfer rate between two electronic states $|i\rangle$ and $|f\rangle$ is expressed by the Fermi's Golden rule as:

$$k_{\mathrm{FGR}} = \frac{2\pi}{\hbar}|V_{if}|^2 F(\Delta E, T), \tag{2}$$

where V_{if} is the electronic coupling between the electronic states, which is considered to be independent of vibrational coordinates, ΔE is the electronic energy difference between the initial and final states, T is the absolute temperature, and $F(\Delta E, T)$ is the Franck-Condon

DOI: 10.1021/acs.jpcc.8b08126

weighted density of states, computable as:

$$F(\Delta E, T) = \frac{1}{Z}\sum_{v_i,v_f} \mathrm{e}^{-\beta E_{v_i}} |\langle v_i | v_f \rangle|^2 \delta\big(E_{v_f} - E_{v_i} - \Delta E\big). \tag{3}$$

Here $\langle v_i | v_f \rangle$ is the Franck-Condon integral, Z is the vibrational partition function of the initial electronic state, $\beta = 1/(k_{\mathrm{B}}T)$, k_{B} being Boltzmann constant and the sum runs over all vibrational states of $|i\rangle$ and $|f\rangle$. The evaluation of $F(\Delta E, T)$ by the infinite summations of eq. 3 poses problems that can be avoided by using the generating function (GF) approach,[36,37] which takes advantage of the integral representation of the Dirac delta function. By using Duschinsky's normal mode transformation,

$$\mathbf{Q}_i = \mathbf{J}\mathbf{Q}_f + \mathbf{K},$$

$F(\Delta E, T)$ can be evaluated in harmonic approximation including the whole sets of nuclear coordinates in computations.[29,38–41]

Second order cumulant approximation

The integral representation of the delta function only holds in the limit of long times, therefore the FGR approach is not fully adequate to treat ultra-fast transitions. For those cases, it would be useful to resort to a formulation taking into account the variation of the rate constant with time, for example the recently developed cumulant expansion of the density matrix.

The cumulant expansion is a well known technique,[42–45] but rather few applications to realistic Hamiltonians have appeared in the literature.[30,31,46,47]

If we consider two electronic state $|i\rangle$ and $|f\rangle$ coupled by constant perturbation V_{if}, the Hamiltonian reads:

$$\mathcal{H} = |i\rangle\, \mathcal{H}_i \langle i| + |f\rangle\, \mathcal{H}_f \langle f| + |i\rangle\, V_{if} \langle f| + c.c. = \mathcal{H}^0 + V, \tag{4}$$

DOI: 10.1021/acs.jpcc.8b08126

where $\mathcal{H}_i$ and $\mathcal{H}_f$ are the vibrational Hamiltonian of the electronic states $|i\rangle$ and $|f\rangle$ respectively and V_{if} is their electronic coupling.

Following the derivations of ref. 43 and 31, the second order cumulant approximation of the population of the initial state is given by:

$$P_i(t) = \exp\left[K_2\left(t\right)\right]$$

, with:

$$K_2(t) = -2\hbar^{-2}\mathrm{ReTr}\int_0^t \mathrm{d}\tau_1 \int_0^{\tau_1} \left\langle i\right| \left[V_I(\tau_2), [V_I(\tau_2), \rho(0)]\right] \left|i\right\rangle \mathrm{d}\tau_2. \tag{5}$$

where the trace is taken over the whole set of the vibrational degrees of freedom of the initial state, and $V_I(s)$ is the interaction representation of the coupling potential V_{if}. The final form of $K_2(t)$ depends on the expression of the initial density of the system $\rho(0)$. If we assume the equilibrium population of the unperturbed initial state, eq. 5 becomes:

$$K_2(t) = -2\hbar^{-2}Z^{-1}\mathrm{Re}\int_0^t \mathrm{d}\tau_1 \int_0^{\tau_1} \mathrm{Tr}\left[\mathrm{e}^{\mathrm{i}\mathcal{H}_i(\tau_2+\mathrm{i}\beta)}V_{if}\mathrm{e}^{-\mathrm{i}\mathcal{H}_f\tau_2}V_{fi}\right]\mathrm{d}\tau_2 \tag{6}$$

For fast hole transfer, one has to consider the thermally equilibrated ground state of the neutral molecule which instantaneously releases an electron. In this case, the initial density for hole transfer is given by:

$$\rho(0) = Z_N^{-1}\left|i\right\rangle \mathrm{e}^{-\beta\mathcal{H}_N}\left\langle i\right|.$$

where $\mathcal{H}_N$ is the vibrational Hamiltonian of the neutral molecule and Z_N its corresponding vibrational partition function, and the second order cumulant average becomes:

$$K_2(t) = -\hbar^{-2}Z_N^{-1}\mathrm{Re}\int_0^t \int_0^t \mathrm{Tr}\left[\mathrm{e}^{-\beta\mathcal{H}_N}\mathrm{e}^{\mathrm{i}\mathcal{H}_i^{\circ}\tau_2}V_{if}\mathrm{e}^{-\mathrm{i}\mathcal{H}_f(\tau_2-\tau_1)}V_{fi}\mathrm{e}^{-\mathrm{i}\mathcal{H}_i\tau_1}\right]\mathrm{d}\tau_1\mathrm{d}\tau_2. \tag{7}$$

This methodology can be easily modified to handle cases where the coupling operator is a function of the nuclear coordinates, see ref. 31.

DOI: 10.1021/acs.jpcc.8b08126

The SOC approach is useful in handling ultra-fast transitions because of the time-dependent nature of the transition rate, furthermore it obtains rate constants approaching a constant value, namely the FGR prediction, in the case of very long times:

$$\lim_{t\to\infty} K_2(t) = \text{constant} = k_{\text{FGR}}. \tag{8}$$

Marcus' theory

If the thermal energy exceeds the vibrational energy, the vibrations can be treated classically and the semiclassical Marcus' theory[48,49] has been widely used for computing hole hopping rates in organic materials.[35,50] When considering hopping between two equal molecules, the net ΔG change is zero, and the charge transfer rate k can be written as:

$$k = \frac{|V|^2}{\hbar}\sqrt{\frac{\pi}{\lambda k_{\text{B}} T}}\exp\left[-\frac{\lambda}{4k_B T}\right] \tag{9}$$

where V is the electronic coupling parameter and λ is the reorganization energy. The latter consists of an intramolecular and an intermolecular contribution, due to equilibrium position changes of the system and of the surrounding medium upon hole transfer. However, computations carried out by using a QM/MM approach with a polarizable force field for naphthalene in its molecular crystal structure showed that the intermolecular reorganization energy is of the order of a few meV;[51] further studies for acenes yield intermolecular reorganization energies typically lower than 0.2 kcal/mol,[50] much smaller than the intramolecular one. For that reason, throughout this work we will consider only the intramolecular part of the reorganization energy.

Mobility calculations

As outlined in the introduction, in this work we adopt a protocol[32] applicable within the framework of the hopping process, where charge transfer takes place by diffusion and the hole

DOI: 10.1021/acs.jpcc.8b08126

hops between neighbouring sites. In the low field limit, the mobility is evaluated resorting to Einstein's formula:

$$\mu = \frac{eD}{k_{\mathrm{B}}T}, \tag{10}$$

where e denotes the elementary charge, k_{B} is the Boltzmann constant, T is the absolute temperature and D is the diffusion coefficient, which is defined as:

$$D = \frac{1}{2n} \lim_{t\to\infty} \frac{\langle r^2 \rangle}{t}, \tag{11}$$

where n is the dimensionality of the system and $\langle r^2 \rangle$ is the mean-square displacement evaluated at $t \to \infty$, i.e. for times long enough that the diffusion regime set out.

For an isotropic system, eq. 11 can be approximated as[33,34,52]

$$D = \frac{1}{2n} \sum_{i}^{N} d_i^2 k_i p_i, \tag{12}$$

where the sum runs over all neighbouring molecules N, d_i being the hopping distance, k_i the relative rate constant, and p_i the hopping probability ($p_i = k_i / \sum_j^N k_j$). When considering the mobility along a single hopping pathway i, eq. 10 can easily be rewritten as:

$$\mu_i = \frac{e d_i^2 k_i}{2 k_{\mathrm{B}} T} \tag{13}$$

This quantity is however a poor descriptor of the actual electronic properties of the material, since it considers a single migration channel, while in actual crystals there are several simultaneous pathways available for charge diffusion. Thus, a better quantity to focus on would be the anisotropic mobility, i.e. the variation of the mobility depending on the orientation of the conductive channel relative to the crystallographic axes, when taking into account all possible charge migration pathways.

Deng et al.[32,33] have developed an appealingly simple, yet effective mobility orientation formula expressing the mobility along a specific conduction direction as the combined effect

DOI: 10.1021/acs.jpcc.8b08126

of all possible hopping pathways. Assuming that there is no correlation between hopping events and that charge motion is a homogenous random walk, the mobility along a given conducting direction on a specific plane in the organic crystal can be computed as

$$\mu_\phi = \frac{e}{2k_\mathrm{B}T} \sum_i k_i d_i^2 P_i \cos^2 \gamma_i \cos^2 (\theta_i - \phi), \tag{14}$$

where γ_i is the angle between the i-th hopping path and the plane of interest and θ_i is the angle of the projected i-th hopping path of different dimer types relative to the reference axis. So the angles between the hopping paths and the conducting channel are $(\theta_i - \phi)$ and $P_i \cos^2 \gamma_i \cos^2 (\theta_i - \phi)$ describes the hopping probability of various dimer types relative to the specific transistor channel (see e.g. top of fig. 1).

In most instances, π-conjugated molecules have a crystal structure with a high-mobility plane, while the mobility perpendicular to this plane is 1-2 orders of magnitude smaller,[7,32] so in the following we will focus on the 2D-transport within the stacked organic layer of interest, evaluating the anisotropic mobility with respect to these layer, so that γ_i is always 0.

Computational details

The crystal structure for all the molecules studied is derived from the Cambridge Structural Database (CSD).[53] The CSD codes are: IUCr A03426 for tetracene, 665900 for pentacene, 605647 for rubrene and 560122 for picene. Equilibrium geometries, normal modes, and vibrational frequencies of pentacene, picene, rubrene, and tetracene in their neutral and cationic forms were obtained at the DFT level using the B3LYP functional with the 6-31+G(d,p) basis set, which has been proved to yield sufficiently accurate results.[54] Dielectric effects have been estimated by using the polarizable continuum model (PCM).[55] According to previous works, we have assumed $\epsilon = 4$ as the average value for the dielectric constants of the bulk materials.[56] The G09 package has been used for electronic wavefunction computations.[57] Franck-Condon weighted densities of states have been computed by

DOI: 10.1021/acs.jpcc.8b08126

using a development version of the MolFC package.[58] Intermolecular reorganization energies have been neglected, because previous computations have shown that they are negligible, at least for the systems considered here.[51] The curvilinear coordinate representation of the normal modes has been adopted to prevent that large displacements of an angular coordinate could reflect into large shifts of the equilibrium positions of the involved bond distances. That unphysical effect is unavoidable when using rectilinear coordinates and requires the use of high order anharmonic potentials for its correction.[40,59–63] The evaluation of the time-dependent rates $K_2(t)$ of eq.s 6 and 7 is based on the coordinate representation of the reduced density matrix; the resulting multidimensional Gaussian type integrals have been evaluated analytically.[64] Time averaged SOC rates used for the evaluation of anisotropic mobilities (reported in table 1) have been obtained interpolating the populations assuming a monoexponentional decay for them. As discussed in the result section, this approximation, whose quality is not known a priori, proves to be effective since it leads to anisotropic mobilities in good agreement with experimental ones. A better approach would be the inclusion of the time dependent kinetic constants for the evaluation of the mobility, but unfortunately they are incompatible with the model here used (eq. 14). Further studies on alternative methods allowing the introduction of time-dependent kinetic constants are ongoing in our group.

Results

Single channel hole mobilities along the most important paths for charge transport in organic semiconductors, at $T = 298$ K are reported in Table 1, alongside with the relative charge transfer rates available from previous work.[30] The electronic coupling elements adopted in computations have been taken from ref.s 33 and 65 and are also reported in Table 1. The molecular arrangements for the various paths are shown in the top of fig.s 1-4, further details are given in ref 30.

The analysis of Table 1 shows that the SOC approximation yields significantly longer transition times than FGR, especially for fast decay rates. For example, for channel 2 of

DOI: 10.1021/acs.jpcc.8b08126

pentacene and channel 3 of tetracene, FGR predicts that the initial state completely decays within 5 fs, whereas SOC approach yields a decay time of about 30 fs. For such ultrafast transitions, the integral representation of Dirac delta function, used in the computation of $F(\Delta E, T)$, could be inappropriate and could lead to significant overestimations of the transition rates. Indeed, as shown elsewhere,[30] quantum dynamics calculation leads to a decay of the initial state in excellent agreement with the one predicted by SOC approach, pointing out that FGR fails in describing ultra-fast charge transfer in these systems.

Table 1: Kinetic constants ($k/10^{13}$ $\mathbf{s}^{-1}$) and mobilities ($\mu/\mathrm{cm}^2\mathbf{V}^{-1}\mathbf{s}^{-1}$) along the different hole channels for the 4 molecules under study. Electronic couplings J (meV) from ref.s 33 and 65.

		Marcus		FGR		$\mathrm{SOC}^a_{\mathrm{eq}}$	
	J	k	μ	k	μ	k	μ
Pentacene (d_1)	20	0.85	0.59	6.54	4.52	2.72	1.88
Pentacene (d_2)	75	12.0	5.46	91.9	41.8	12.3	5.60
Pentacene (d_3)	32	2.19	1.01	16.7	7.55	4.77	2.16
Tetracene (d_1)	17	0.49	0.25	5.17	2.64	2.32	1.19
Tetracene (d_2)	1	0.002	0.001	0.02	0.007	0.005	0.003
Tetracene (d_3)	70	8.26	3.72	87.7	39.5	11.3	5.09
Picene (d_1)	66	2.94	1.63	7.08	3.92	6.81	3.77
Picene (d_2)	70	3.31	2.44	7.96	5.87	7.63	5.60
Picene (d_3)	54	1.97	1.02	4.74	2.44	4.57	2.32
Rubrene (d_1)	19	0.38	0.47	0.44	0.543	0.41	0.506
Rubrene (d_2)	19	0.38	0.47	0.44	0.543	0.41	0.506
Rubrene (d_3)	89	8.41	8.41	9.74	9.75	9.00	9.01

[a] initial state from the equilibrium thermal distribution of the cationic state. See ref 30 for data referring to the equilibrium thermal distribution of the neutral state.

Figure 1 shows on the top the hopping paths and the angles of the paths with respect to the reference axis a (numerical values are reported in the caption of the figure) for pentacene. All hopping paths are in the ab plane. Using eq. 14 with the data of Table 1 yields the angular dependence of hole mobility of pentacene in single crystal molecular arrangements, shown in the bottom left of Figure 1; there the experimental results of Lee et al.[66] are also reported.

DOI: 10.1021/acs.jpcc.8b08126

The crystal orientation was not determined in the experiment, therefore the experimental data have been rotated to best fit with theoretical predictions.[33]

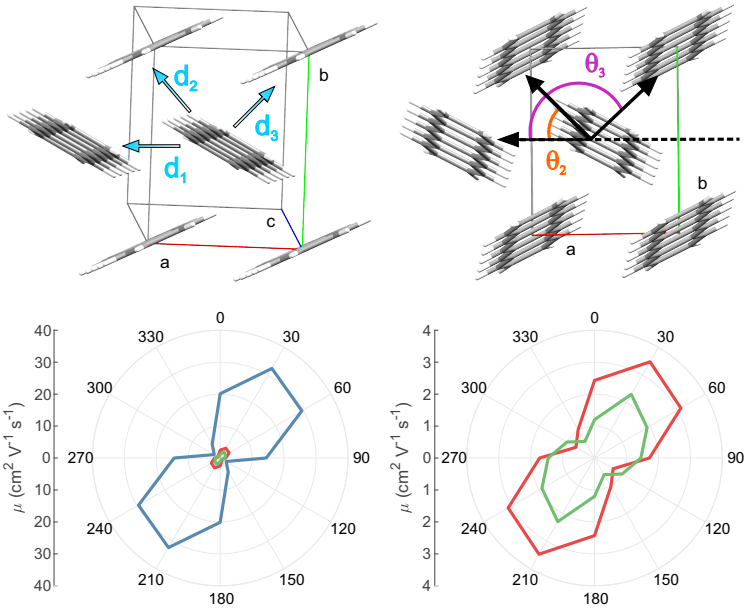

Figure 1: Top: hole hopping paths in pentacene single crystal (left) and their projection to a conducting channel in the ab plane(right); Angles relative to the reference axis a are: $\theta_1 = 0$, $\theta_2 = 47.32$, $\theta_3 = 126.47$. Bottom left: polar plot of experimental (green line) and predicted anisotropic hole mobility of pentacene using FGR (blue line), SOC (red line); bottom right: a magnified views of experimental and SOC mobilities. Experimental results from ref.s 33 and 66.

Figure 1 shows that FGR mobilities are significantly larger, about one order of magnitude, than SOC ones, the latter being in excellent agreement with the experimental results.[66,67] Noteworthy, a significantly higher mobility, 35 $cm^2V^{-1}s^{-1}$ at room temperature increasing up to 58 $cm^2V^{-1}s^{-1}$ at 225 K, has been measured by Jurchescu et al. in highly purified single crystal of pentacene, in which 6,13-pentacenequinone traps were removed by vacuum sublimation.[26] According to our computations, such a high mobility is not compatible with the simple hopping mechanism and possibly coherence effects have to play a role, as indeed previously inferred on the basis of the observed temperature dependence of mobility.[26]

Similar results have been obtained for tetracene, for which the anisotropic mobility evaluated with respect to the reference axis a is reported in Figure 2. For tetracene, predicted mobilities are significantly higher than their experimental counterpart, even SOC predictions. That is possibly due to the fact that experimental samples unavoidably contain impurities,

DOI: 10.1021/acs.jpcc.8b08126

defects and dislocations which have not been considered in our model. Indeed, more recent experimental measurements[68] over purer samples have reported significantly higher mobilities, up to 2.4 $cm^2V^{-1}s^{-1}$.

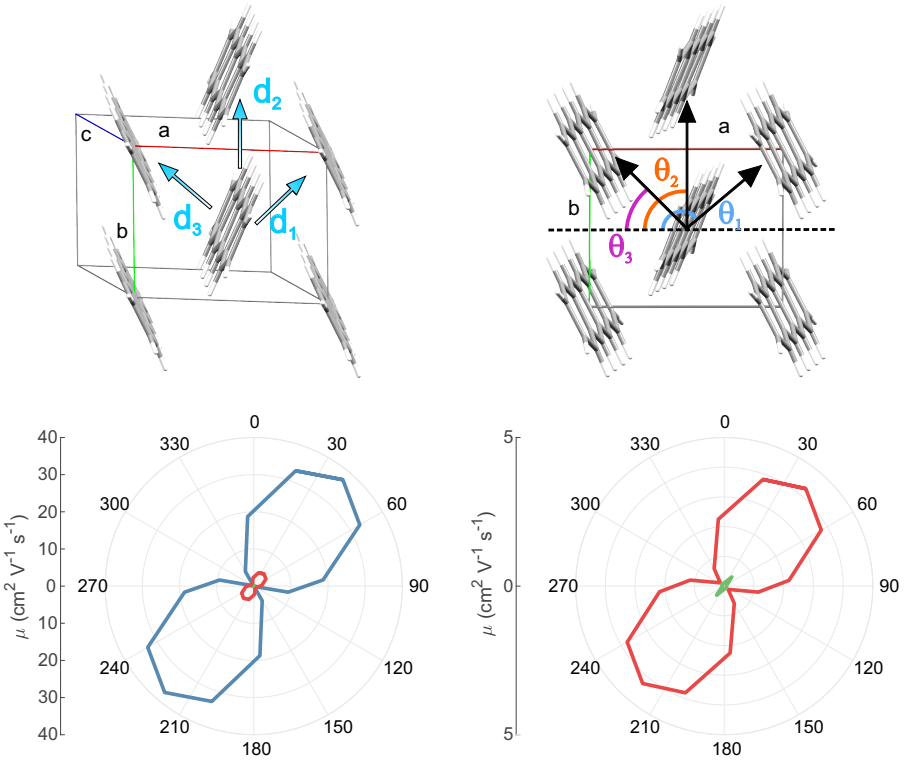

Figure 2: Top: hole hopping paths in tetracene single crystal (left) and their projection to a conducting channel in the *ab* plane(right); Angles relative to the reference axis *a* are: $\theta_1 = 141.67$, $\theta_2 = 90.00$, $\theta_3 = 39.95$. Bottom: polar plot of experimental (green line) and predicted anisotropic hole mobility of tetracene using FGR (blue line), SOC (red line); on the right a zoom showing only experimental and SOC mobility. Experimental results from ref. 69

Rubrene and picene behave differently: since charge transfer occurs on a longer timescale, it is expected that FGR should lead to reliable mobility values. Indeed, as shown in table 1, for these molecules FGR values are in excellent agreement with SOC ones.

In Figure 3, the anisotropic mobility for rubrene evaluated with respect to the reference axis *c* is reported, showing that for this system FGR and SOC anisotropic predictions are almost indistinguishable from each other, both being in good agreement with experimental results.

Finally, in fig. 4 we report the anisotropic mobility for picene, once again displaying a

DOI: 10.1021/acs.jpcc.8b08126

good agreement between FGR and SOC. Unfortunately, to the best of our knowledge, no experimental results have been reported yet in the literature to be compared with our data.

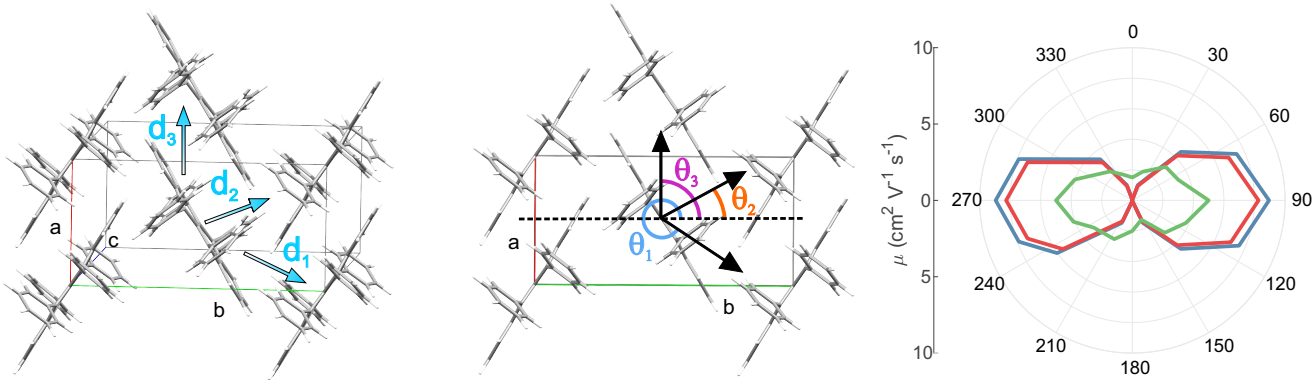

Figure 3: Hole hopping paths in rubrene single crystal (left) and their projection to a conducting channel in the ab plane(middle); Angles relative to the reference axis b are: $\theta_1 = 331.70$, $\theta_2 = 28.30$, $\theta_3 = 90.0$. On the right, the polar plot of experimental (green line) and predicted anisotropic hole mobility of pentacene using FGR (blue line), SOC (red line). Experimental results from ref. 67

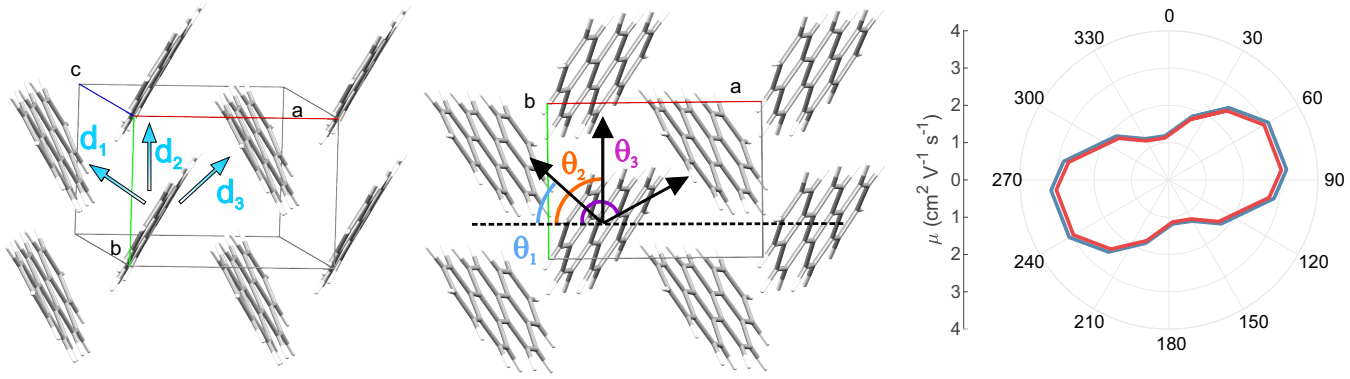

Figure 4: Hole hopping paths in picene single crystal (left) and their projection to a conducting channel in the ab plane(middle); Angles relative to the reference axis a are: $\theta_1 = 37.30$, $\theta_2 = 87.10$, $\theta_3 = 142.05$ degrees. On the right, the polar plot of predicted anisotropic hole mobility of pentacene using FGR (blue line), SOC (red line).

Anisotropic mobilities obtained starting from Marcus' rate constants have not been reported in the figures since they are very similar to SOC ones, as table 1 shows. On the basis of this analysis, one can conclude that Marcus approach is adequate for the evaluation of the mobilities at room temperature. However it fails when used to reproduce the experimental temperature dependence of the mobility, as shown in fig. 5, where the predicted hole mobilities of pentacene (top) and rubrene (bottom) along the fastest paths at different

DOI: 10.1021/acs.jpcc.8b08126

temperatures are reported. Both FGR and SOC approaches yield a hole mobility which decreases as temperature increase for both the systems. That behavior can be rationalized on the basis of the temperature dependence of the Franck-Condon weighted density of states. As T decreases the value of $F(\Delta E, T)$ at $\Delta E = 0$ increases, because of the decreasing populations of low frequency vibrational modes. It is worth noting that somewhat contradictory experimental results are available for pentacene: in thin films different behaviors have been observed, including an almost temperature independent device mobility,[70–72] whereas in single crystals hole mobility was observed to decrease upon increasing temperature.[26]

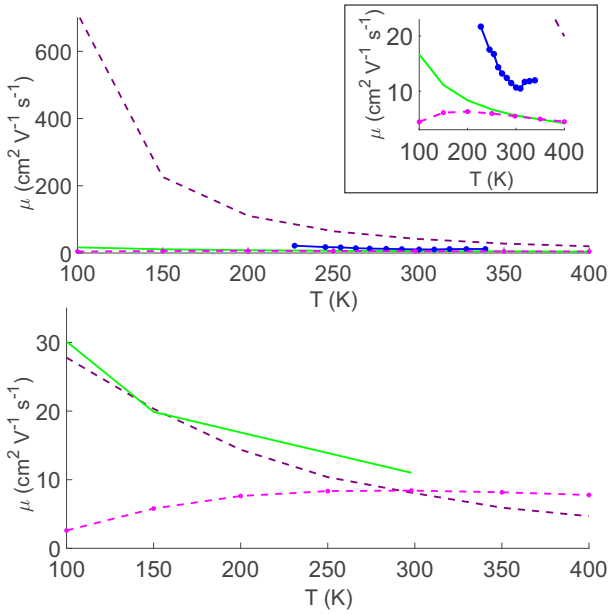

Figure 5: Predicted hole mobilities as a function of the temperature for: pentacene (top) and rubrene (bottom). Green full line: SOC approach; purple dashed line: FGR; pink dashed line with dots: Marcus formula; blue full line: experimental values from ref. 26. Inset: detailed comparison of experimental and SOC predicted mobilities for pentacene.

However, SOC temperature dependence of mobility is in good agreement with the experimental trend reported in ref. 26 although predicted and observed mobilities are somewhat different. The discrepancy between experimental and theoretical data increases as the temperature decreases, possibly because coherence effects (not included in our model) play a larger role at lower temperatures.

As concerns rubrene, two transport regimes have been observed: (i) an intrinsic regime,

DOI: 10.1021/acs.jpcc.8b08126

occurring at higher temperatures, where the mobility increases with decreasing temperature and (*ii*) a shallow-trap-dominated regime, where the mobility decreases rapidly with cooling.[73,74] The observed mobility in the intrinsic regime varies from ≈ 25 cm^2 V^{-1} s^{-1} at 175 K up to ≈ 10 cm^2 V^{-1} s^{-1} at 300 K, in good agreement with our predictions, as shown in Figure 5.

For both pentacene and rubrene, Marcus' formula predicts a thermally activated behaviour, leading to mobilities increasing as T increases, in contrast with experimental data. Marcus' formula failure at low temperatures is somewhat expected, since it is treats molecular modes classically, an approximation valid only at relatively high temperatures.

Conclusions

Angle resolved hole mobilities for pentacene, tetracene, rubrene, and picene in single crystal geometrical arrangements have been computed by first principles, upon assuming that hole transport occurs by the hopping mechanism. The mobility orientation formula developed in ref.s 32 and 33 has been employed for the anisotropic mobility evaluation, using hole transfer rates obtained by three different methods: the semiclassical Marcus approach, the Fermi Golden Rule, and the second order expansion of the reduced density matrix (SOC).

Predicted mobilities by the SOC approach are in good agreement with experimental data, although they appear to be slightly overestimated. That is possibly due to the influence of surface contamination, grain boundaries, defects, etc. which have been omitted in simulations but are always present in real samples.[14,75,76] Therefore, the SOC approach appears to provide a computationally economical and reliable way for estimating hole transfer mobilities, including their temperature dependence, considering the whole set of intramolecular vibrational coordinates. That approach can also handle cases in which the Fermi Golden Rule is inadequate, i.e. ultrafast hole transfer processes, occurring in molecular systems exhibiting strongly peaked Franck-Condon weighted density of states.[30] Marcus' semiclassical

DOI: 10.1021/acs.jpcc.8b08126

approach can provide qualitatively correct values of mobilities at room temperature, but it is unable to provide reliable temperature dependencies because it cannot account for tunnelling effects dominating at low temperatures.

Acknowledgement

The financial supports of the University of Salerno and of the European Community (PON Relight project) are gratefully acknowledged.

References

(1) Wang, C.; Dong, H.; Jiang, L.; Hu, W. Organic semiconductor crystals. *Chem. Soc. Rev.* **2018**, *47*, 422–500.

(2) Wu, J.; Lan, Z.; Lin, J.; Huang, M.; Huang, Y.; Fan, L.; Luo, G. Electrolytes in Dye-Sensitized Solar Cells. *Chem. Rev.* **2015**, *115*, 2136–2173.

(3) Scholz, S.; Kondakov, D.; Lüssem, B.; Leo, K. Degradation Mechanisms and Reactions in Organic Light-Emitting Devices. *Chem. Rev.* **2015**, *115*, 8449–8503.

(4) Mei, J.; Diao, Y.; Appleton, A. L.; Fang, L.; Bao, Z. Integrated Materials Design of Organic Semiconductors for Field-Effect Transistors. *J. Am. Chem. Soc.* **2013**, *135*, 6724–6746.

(5) Lee, S. M.; Kwon, J. H.; Kwon, S.; Choi, K. C. A Review of Flexible OLEDs Toward Highly Durable Unusual Displays. *IEEE Trans. Electron Devices* **2017**, *64*, 1922–1931.

(6) Lu, L.; Zheng, T.; Wu, Q.; Schneider, A. M.; Zhao, D.; Yu, L. Recent Advances in Bulk Heterojunction Polymer Solar Cells. *Chem. Rev.* **2015**, *115*, 12666–12731.

(7) Fratini, S.; Ciuchi, S.; Mayou, D.; De Laissardière, G. T.; Troisi, A. A map of high-mobility molecular semiconductors. *Nat. Mater.* **2017**, *16*, 998–1002.

DOI: 10.1021/acs.jpcc.8b08126

(8) Stehr, V.; Fink, F., R.; Tafipolski, M.; Deibel, C.; Engels, B. Comparison of Different Rate Constant Expressions for the Prediction of Charge and Energy Transport in Oligoacenes. *Comput. Mol. Sci. 6*, 694–720.

(9) Troisi, A.; Orlandi, G. Charge-Transport Regime of Crystalline Organic Semiconductors: Diffusion Limited by Thermal Off-Diagonal Electronic Disorder. *Phys. Rev. Lett.* **2006**, *96*, 086601.

(10) Troisi, A. Prediction of the Absolute Charge Mobility of Molecular Semiconductors: the Case of Rubrene. *Adv. Mat.* **2007**, *19*, 2000–2004.

(11) Ortmann, F.; Bechstedt, F.; Hannewald, K. Charge Transport in Organic Crystals: Theory and Modelling. *Phys. Stat. Sol. (b)* **2011**, *248*, 511–525.

(12) Ren, J.; Vukmirović, N.; Wang, L.-W. Nonadiabatic Molecular Dynamics Simulation for Carrier Transport in a Pentathiophene Butyric Acid Monolayer. *Phys. Rev. B* **2013**, *87*, 205117.

(13) Heck, A.; Kranz, J. J.; Kubar, T.; Elstner, M. Multi-Scale Approach to Non-Adiabatic Charge Transport in High-Mobility Organic Semiconductors. *J. Chem. Theory Comput.* **2015**, *11*, 5068–5082.

(14) Spencer, J.; Gajdos, F.; Blumberger, J. FOB-SH: Fragment Orbital-Based Surface Hopping for Charge Carrier Transport in Organic and Biological Molecules and Materials. *J. Chem. Phys.* **2016**, *145*, 064102.

(15) Cheng, Y. C.; Silbey, R. J.; da Silva Filho, D. A.; Calbert, J. P.; Cornil, J.; Brédas, J. L. Three-Dimensional Band Structure and Bandlike Mobility in Oligoacene Single Crystals: A Theoretical Investigation. *J. Chem. Phys.* **2003**, *118*, 3764–3774.

(16) Simone, F.; Didier, M.; Sergio, C. The Transient Localization Scenario for Charge Transport in Crystalline Organic Materials. *Adv. Funct. Mat. 26*, 2292–2315.

DOI: 10.1021/acs.jpcc.8b08126

(17) Troisi, A. Dynamic Disorder in Molecular Semiconductors: Charge Transport in Two Dimensions. *J. Chem. Phys.* **2011**, *134*, 034702.

(18) Wang, L.; Beljonne, D. Flexible Surface Hopping Approach to Model the Crossover from Hopping to Band-like Transport in Organic Crystals. *J. Phys. Chem. Lett.* **2013**, *4*, 1888–1894.

(19) Lee, C. K.; Moix, J.; Cao, J. Coherent Quantum Transport in Disordered Systems: a Unified Polaron Treatment of Hopping and Band-like Transport. *J. Chem. Phys.* **2015**, *142*, 164103.

(20) De Filippis, G.; Cataudella, V.; Mishchenko, A. S.; Nagaosa, N.; Fierro, A.; de Candia, A. Crossover from Super- to Subdiffusive Motion and Memory Effects in Crystalline Organic Semiconductors. *Phys. Rev. Lett.* **2015**, *114*, 086601.

(21) Chen, D.; Ye, J.; Zhang, H.; Zhao, Y. On the Munn-Silbey Approach to Polaron Transport with Off-Diagonal Coupling and Temperature-Dependent Canonical Transformations. *J. Phys. Chem. B* **2011**, *115*, 5312–5321.

(22) Borrelli, R.; Capobianco, A.; Landi, A.; Peluso, A. Vibronic Couplings and Coherent Electron Transfer in Bridged Systems. *Phys. Chem. Chem. Phys.* **2015**, *17*, 30937–30945.

(23) Heck, A.; Kranz, J. J.; Elstner, M. Simulation of Temperature-Dependent Charge Transport in Organic Semiconductors with Various Degrees of Disorder. *J. Chem. Theory Comput.* **2016**, *12*, 3087–3096.

(24) Landi, A.; Troisi, A. Rapid Evaluation of Dynamic Electronic Disorder in Molecular Semiconductors. *J. Phys. Chem. C* **2018**, http://dx.doi.org/10.1021/acs.jpcc.8b05511.

(25) Ciuchi, S.; Fratini, S. Electronic transport and quantum localization effects in organic semiconductors. *Phys. Rev. B* **2012**, *86*, 245201.

DOI: 10.1021/acs.jpcc.8b08126

(26) Jurchescu, O. D.; Baas, J.; Palstra, T. T. M. Effect of Impurities on the Mobility of Single Crystal Pentacene. *Appl. Phys. Lett.* **2004**, *84*, 3061–3063.

(27) Vehoff, T.; Baumeier, B.; Troisi, A.; Andrienko, D. Charge Transport in Organic Crystals: Role of Disorder and Topological Connectivity. *J. Am. Chem. Soc.* **2010**, *132*, 11702–11708.

(28) Wang, L.; Nan, G.; Yang, X.; Peng, Q.; Li, Q.; Shuai, Z. Computational Methods for Design of Organic Materials with High Charge Mobility. *Chem. Soc. Rev.* **2010**, *39*, 423–434.

(29) Nan, G.; Yang, X.; Wang, L.; Shuai, Z.; Zhao, Y. Nuclear Tunneling Effects of Charge Transport in Rubrene, Tetracene, and Pentacene. *Phys. Rev. B* **2009**, *79*, 115203.

(30) Landi, A.; Borrelli, R.; Capobianco, A.; Velardo, A.; Peluso, A. Hole Hopping Rates in Organic Semiconductors: A Second-Order Cumulant Approach. *J. Chem. Theory Comput.* **2018**, *14*, 1594–1601.

(31) Borrelli, R.; Peluso, A. Quantum Dynamics of Radiationless Electronic Transitions Including Normal Modes Displacements and Duschinsky Rotations: A Second-Order Cumulant Approach. *J. Chem. Theory Comput.* **2015**, *11*, 415–422.

(32) Deng, W.; Sun, L.; Huang, J.; Chai, S.; Wen, S.; Han, K. Quantitative Prediction of Charge Mobilities of π-Stacked Systems by First-Principles Simulation. *Nature Protocols* **2015**, *10*, 632–642.

(33) Wen, S.-H.; Li, A.; Song, J.; Deng, W.-Q.; Han, K.-L.; Goddard, W. A. First-Principles Investigation of Anistropic Hole Mobilities in Organic Semiconductors. *J. Phys. Chem. B* **2009**, *113*, 8813–8819.

(34) Deng, W.-Q.; Goddard, W. A. Predictions of Hole Mobilities in Oligoacene Organic

DOI: 10.1021/acs.jpcc.8b08126

Semiconductors from Quantum Mechanical Calculations. *J. Phys. Chem. B* **2004**, *108*, 8614–8621.

(35) Yavuz, I.; Martin, B. N.; Park, J.; Houk, K. N. Theoretical Study of the Molecular Ordering, Paracrystallinity, And Charge Mobilities of Oligomers in Different Crystalline Phases. *J. Am. Chem. Soc.* **2015**, *137*, 2856–2866.

(36) Lax, M. The Franck-Condon Principle and Its Application to Crystals. *J. Chem. Phys.* **1952**, *20*, 1752–1760.

(37) Kubo, R.; Toyozawa, Y. Application of the Method of Generating Function to Radiative and Non-Radiative Transitions of a Trapped Electron in a Crystal. *Prog. Theor. Phys.* **1955**, *13*, 160–182.

(38) Borrelli, R.; Peluso, A. The Temperature Dependence of Radiationless Transition Rates from Ab Initio Computations. *Phys. Chem. Chem. Phys.* **2011**, *13*, 4420–4426.

(39) Borrelli, R.; Capobianco, A.; Peluso, A. Generating Function Approach to the Calculation of Spectral Band Shapes of Free-Base Chlorin Including Duschinsky and Herzberg-Teller Effects. *J. Phys. Chem. A* **2012**, *116*, 9934–9940.

(40) Borrelli, R.; Capobianco, A.; Peluso, A. Franck-Condon Factors: Computational Approaches and Recent Developments. *Can. J. Chem.* **2013**, *91*, 495–504.

(41) Borrelli, R.; Peluso, A. Elementary Electron Transfer Reactions: from Basic Concepts to Recent Computational Advances. *WIREs: Comput. Mol. Sci.* **2013**, *3*, 542–559.

(42) Kubo, R. Stochastic Liouville Equations. *J. Math. Phys.* **1963**, *4*, 174–183.

(43) Mukamel, S. *Principles of Nonlinear Optical Spectroscopy*; Oxford University Press: USA, 1995; Chapter 3.

(44) Breuer, F., H.-P.; Petruccione *The Theory of Open Quantum Systems*; Oxford University Press: USA, 2002; Chapter 3.

DOI: 10.1021/acs.jpcc.8b08126

(45) Van Kampen, N. G. A Cumulant Expansion for Stochastic Linear differential Equations. I. *Physica* **1974**, *74*, 215–238.

(46) Izmaylov, A. F.; Mendive-Tapia, D.; Bearpark, M. J.; Robb, M. A.; Tully, J. C.; Frisch, M. J. Nonequilibrium Fermi Golden Rule for Electronic Transitions through Conical Intersections. *J. Chem. Phys.* **2011**, *135*, 234106.

(47) Pereverzev, A.; Bittner, E. R. Time-convolutionless master equation for mesoscopic electron-phonon systems. *J. Chem. Phys.* **2006**, *125*, 104906.

(48) Marcus, R. A. On the Theory of Oxidation-Reduction Reactions Involving Electron Transfer. I. *J. Chem. Phys.* **1956**, *24*, 966–978.

(49) Marcus, R. A. Electron Transfer Reactions in Chemistry. Theory and Experiment. *Rev. Mod. Phys.* **1993**, *65*, 599–610.

(50) McMahon, D. P.; Troisi, A. Evaluation of the External Reorganization Energy of Polyacenes. *J. Phys. Chem. Lett.* **2010**, *1*, 941–946.

(51) Norton, J. E.; Brédas, J.-L. Polarization Energies in Oligoacene Semiconductor Crystals. *J. Am. Chem. Soc.* **2008**, *130*, 12377–12384.

(52) Zhang, Y.; Cai, X.; Bian, Y.; Li, X.; Jiang, J. Heteroatom Substitution of Oligothienoacenes: From Good p-Type Semiconductors to Good Ambipolar Semiconductors for Organic Field-Effect Transistors. *J. Phys. Chem. C* **2008**, *112*, 5148–5159.

(53) Groom, C. R.; Bruno, I. J.; Lightfoot, M. P.; Ward, S. C. The Cambridge structural database. *Acta Cryst. B* **2016**, *72*, 171–179.

(54) Capobianco, A.; Caruso, T.; Peluso, A. Hole Delocalization over Adenine Tracts in Single Stranded DNA Oligonucleotides. *Phys. Chem. Chem. Phys.* **2015**, *17*, 4750–4756.

DOI: 10.1021/acs.jpcc.8b08126

(55) Miertiuš, S.; Scrocco, E.; Tomasi, J. Electrostatic Interaction of a Solute with a Continuum. A Direct Utilization of Ab Initio Molecular Potentials for the Prevision of Solvent effects. *Chem. Phys.* **1981**, *55*, 117–129.

(56) D'Avino, G.; Muccioli, L.; Zannoni, C.; Beljonne, D.; Soos, Z. G. Electronic Polarization in Organic Crystals: A Comparative Study of Induced Dipoles and Intramolecular Charge Redistribution Schemes. *J. Chem. Theory Comput.* **2014**, *10*, 4959–4971.

(57) Frisch, M. J.; Trucks, G. W.; Schlegel, H. B.; Scuseria, G. E.; Robb, M. A.; Cheeseman, J. R.; Scalmani, G.; Barone, V.; Mennucci, B.; Petersson, G. A. et al. Gaussian 09 Revision D.01. Gaussian Inc. Wallingford CT 2009.

(58) Borrelli, R.; Peluso, A. MolFC: A program for Franck-Condon integrals calculation. Package available online at `http://www.theochem.unisa.it`.

(59) Borrelli, R.; Peluso, A. The Vibrational Progressions of the N ← V Electronic Transition of Ethylene. A Test Case for the Computation of Franck-Condon Factors of Highly Flexible Photoexcited Molecules. *J. Chem. Phys.* **2006**, *125*, 194308–8.

(60) Borrelli, R.; Peluso, A. Erratum: "The Vibrational Progressions of the N ← V Electronic Transition of Ethylene: A Test Case for the Computation of Franck-Condon Factors of Highly Flexible Photoexcited Molecules". *J. Chem. Phys.* **2013**, *139*, 159902–1.

(61) Peluso, A.; Borrelli, R.; Capobianco, A. Photoelectron Spectrum of Ammonia, a Test Case for the Calculation of Franck–Condon Factors in Molecules Undergoing Large Geometrical Displacements upon Photoionization. *J. Phys. Chem. A* **2009**, *113*, 14831–14837.

(62) Peluso, A.; Borrelli, R.; Capobianco, A. Correction to "Photoelectron Spectrum of Ammonia, a Test Case for the Calculation of Franck-Condon Factors in Molecules Undergoing Large Geometrical Displacements upon Photoionization". *J. Phys. Chem. A* **2013**, *117*, 10985–10985.

DOI: 10.1021/acs.jpcc.8b08126

(63) Capobianco, A.; Borrelli, R.; Noce, C.; Peluso, A. Franck-Condon Factors in Curvilinear Coordinates: The Photoelectron Spectrum of Ammonia. *Theor. Chem. Acc.* **2012**, *131*, 1181.

(64) Borrelli, R.; Peluso, A. Quantum Dynamics of Electronic Transitions with Gauss-Hermite Wave Packets. *J. Chem. Phys.* **2016**, *144*, 114102.

(65) Bakulin, A. A.; Lovrincic, R.; Yu, X.; Selig, O.; Bakker, H. J.; Rezus, Y. L. A.; Nayak, P. K.; Fonari, A.; Coropceanu, V.; Brédas, J.-L. et al. Mode-selective vibrational modulation of charge transport in organic electronic devices. *Nat. Commun.* **2015**, *6*, 7880.

(66) Lee, J. Y.; Roth, S.; Park, Y. W. Anisotropic Field Effect Mobility in Single Crystal Pentacene. *Appl. Phys. Lett.* **2006**, *88*, 252106.

(67) Ling, M.; Reese, C.; Briseno, A. L.; Bao, Z. Non-Destructive Probing of the Anisotropy of Field-Effect Mobility in the Rubrene Single Crystal. *Synth. Met.* **2007**, *157*, 257 – 260.

(68) Reese, C.; Chung, W.-J.; Ling, M.-m.; Roberts, M.; Bao, Z. High-Performance Microscale Single-Crystal Transistors by Lithography on an Elastomer Dielectric. *Appl. Phys. Lett.* **2006**, *89*, 202108.

(69) Xia, Y.; Kalihari, V.; Frisbie, C. D.; Oh, N. K.; Rogers, J. A. Tetracene Air-Gap Single-Crystal Field-Effect Transistors. *Appl. Phys. Lett.* **2007**, *90*, 162106.

(70) Sarker, B. K.; Khondaker, S. I. Lower Activation Energy in Organic Field Effect Transistors with Carbon Nanotube Contacts. *Solid State Electron.* **2014**, *99*, 55 – 58.

(71) Zhu, M.; Liang, G.; Cui, T.; Varahramyan, K. Temperature and Field Dependent Mobility in Pentacene-Based Thin Film Transistors. *Solid State Electron.* **2005**, *49*, 884 – 888.

DOI: 10.1021/acs.jpcc.8b08126

(72) Nelson, S. F.; Lin, Y.-Y.; Gundlach, D. J.; Jackson, T. N. Temperature-Independent Transport in High-Mobility Pentacene Transistors. *Appl. Phys. Lett.* **1998**, *72*, 1854–1856.

(73) Podzorov, V.; Menard, E.; Borissov, A.; Kiryukhin, V.; Rogers, J. A.; Gershenson, M. E. Intrinsic Charge Transport on the Surface of Organic Semiconductors. *Phys. Rev. Lett.* **2004**, *93*, 086602.

(74) Podzorov, V.; Menard, E.; Rogers, J. A.; Gershenson, M. E. Hall Effect in the Accumulation Layers on the Surface of Organic Semiconductors. *Phys. Rev. Lett.* **2005**, *95*, 226601.

(75) Jurchescu, O.; Popinciuc, M.; van Wees, B.; Palstra, T. Interface-Controlled, High-Mobility Organic Transistors. *Adv. Mat.* **2007**, *19*, 688–692.

(76) Bashir, A.; Heck, A.; Narita, A.; Feng, X.; Nefedov, A.; Rohwerder, M.; Mullen, K.; Elstner, M.; Woll, C. Charge Carrier Mobilities in Organic Semiconductors: Crystal Engineering and the Importance of Molecular Contacts. *Phys. Chem. Chem. Phys.* **2015**, *17*, 21988–21996.

DOI: 10.1021/acs.jpcc.8b08126

Graphical TOC Entry